

Soheila Riahi

Thermal Behaviour of High Temperature PCMs under a Periodic Heat Transfer Fluid Flow Reversal

Soheila Riahi¹, Wasim Saman¹, Frank Bruno¹, Martin Belusko¹

¹*Barbara Hardy Institute, University of South Australia, Mawson Lakes Campus, SA, 5095, Australia*

E-mail: soheila.riahi@mymail.unisa.edu.au

Abstract

Latent heat thermal energy storage units need to provide a timely response at adequate heat transfer rates to comply with the plant design requirements. This paper presents a method to enhance the heat transfer rate and heat storage /release capacity of a latent heat storage unit. It involves reversing periodically the direction of heat transfer fluid within a specific time interval affecting the phase change boundary over the phase change process. A system incorporating phase change material (PCM) comprising two tubes in a parallel flow arrangement of a shell and tube configuration was investigated numerically, using Fluent. The heat transfer fluid flows through the tubes and PCM is confined between them. Results show that the periodic oscillation of heat transfer fluid flow direction imposes a periodic temperature profile at the tube-PCM interface and consequently affects the phase front which is the heat transfer area in a phase change process. The heat transfer rate in the melting process was enhanced after 40% melt fraction due to the resonance of natural convection. The heat transfer rate was improved in the discharging process after 75% phase change due to higher heat transfer area and the impact of the phase front. In both phase change processes, oscillating the heat transfer fluid flow direction results in a lower temperature gradient in space and time, lower peak temperatures in the melting process, and achieved high heat transfer rates which can be directly applicable to PCM energy storage in concentrated solar power plants.

1. Introduction

Shell and tube and plate heat exchangers are extensively used in different applications of fluid to fluid heat transfer. While the thermal behavior of fluids in those applications is well understood, further research is needed in the scope of design and optimisation of a shell and tube unit or a plate heat exchanger as latent heat thermal energy storage (LHTES) when the phase change of one of the fluids is used as an effective means of thermal energy storage. The design criteria for a LHTES unit are governed by the upstream (solar field) conditions and the downstream conditions (power block) which determine the heat transfer fluid (HTF) inlet and outlet temperatures and also the selection of PCM. The main objectives in the design and optimisation of a LHTES unit are the highest volume fraction of PCM for highest energy storage density, and the lowest temperature gradient in space and time to achieve the highest exergy recovery. Moreover, this system should store and release energy in the time interval that is required in a concentrated solar power (CSP) plant, meaning that the power density of the system is another important factor in conjunction with the energy density of the unit.

There has been some research efforts in the field of periodic boundary conditions and the impact on the convection heat transfer. In an analytical and numerical investigation by Lage and Bejan (1993), the impact of periodic heat flux on one side of a cavity on the natural convection was explored. Results showed a higher heat transfer rate due to the resonance of natural convection heat transfer at a specific frequency close to the natural frequency of the system depending on the geometry and thermophysical properties of the fluid. In two other numerical studies by Antohe and Lage (1996, 1997), the impact of the pulsating boundary condition and Prandtl number (Pr) of the fluid were investigated.

Furthermore, in a limited research effort, the impact of periodic boundary condition in a melting process has been investigated. In two studies by Ho and Cho (1993), the impact of an oscillating temperature boundary condition on the natural convection in the melting processes of tin and ice in a vertical enclosure were investigated. Results of the first study showed a minor effect of the periodic boundary condition on the heat transfer rate whereas the results of the second study showed a higher heat transfer rate in comparison to the fixed boundary condition.

In a recent numerical study by Krishnan et al. (2006), the impact of an oscillating temperature on the melting front evolution was investigated. A PCM with $Pr=50$ confined in a rectangular enclosure with and without metal foam was used to study the effect of Rayleigh number (Ra), Stefan number (Ste) and the frequency of the pulsed temperature. The authors found that an oscillating heat source has profound impact on the thermal behavior of PCM during a melting process.

In all of the studies in the field of periodic boundary condition, the amount of heat source or the imposed temperature on the boundary of the system were changed. In this paper, a method is proposed to enhance the thermal performance of a LHTES system using the periodic boundary condition without changing the magnitude of the heat source. The higher performance of the system can be achieved by adding a few extra elements to the control system without extra complication in the fabrication of the LHTES unit.

2. Methodology

Numerical modeling, using ANSYS Fluent (ANSYS, 2015), was performed to predict the thermal behavior of the PCM during different phase change processes under different boundary conditions at the tube-PCM interface. In the melting and solidification option in Fluent, latent heat transfer at the liquid/solid interface is calculated using the enthalpy-porosity method with a fixed grid proposed by Voller et al. (1989). Using this method, the time dependent Navier-Stokes equations are solved. The PCM domain is considered as a porous medium where porosity is equal to 1 in the liquid region and it is equal to zero in the solid region. The mushy zone where latent heat transfer occurs, porosity changes between zero and 1. The phase front is tracked including latent heat transfer in the energy equation. A sink term is added to the momentum equation to consider zero velocity for the solid region. More detail can be found in the ANSYS Fluent (ANSYS, 2015).

For this study, a model which was developed by Riahi et al. (2016) in Fluent and validated with experimental data (Jones et al., 2006) was used. For the validation purpose, the model was used to predict the thermal behavior of a PCM during the inward melting process in a vertical cylinder with fixed temperature at the outer surface. Comprehensive validation of the model were performed including the comparison of temperatures at different locations, melt front locations and melt fraction against well prepared measured data provided by Jones et al. (2006). The predicted results showed good agreement with the experimental results. The

assumption for the model were; same density for solid and liquid phases, constant density unless in the gravity force term in the momentum equation where a linear density-temperature relation was assumed as Boussinesq approximation, and natural convection flow assumed to be laminar and inviscid. More detail can be found in (Riahi et al., 2016).

3. PCM system, geometry and grid

In the LHTES model, sodium nitrate as the PCM and air as the HTF were used in a shell and tube heat exchanger with parallel flow configuration. In this system, the HTF flows through tubes in parallel and melts/solidifies PCM in the shell. The melting temperature of the PCM, $T_m = 306.8^\circ\text{C}$, and all other thermophysical properties, including $Pr = 9.2$ were acquired from a study by Lan and Yang (1998). The specification of this model was acquired from a lab scale shell and tube LHTES unit.

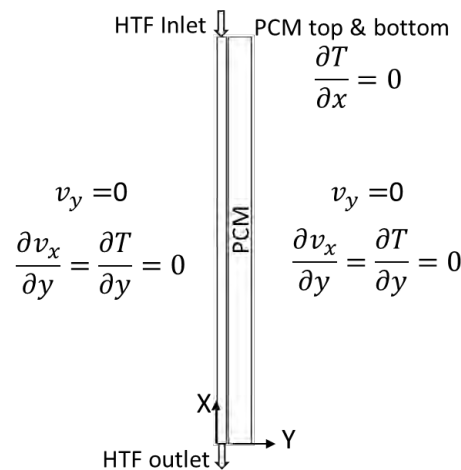


Figure 1: Schematic of the model, including boundary conditions

Two tubes as an element of a parallel flow configuration in the shell and tube LHTES unit was selected to study the thermal behaviour of PCM in charging and discharging processes. The height of the tubes and PCM is $Z = 0.55$ m, the width is 0.06 m (tube diameter equal to 0.0081 m, PCM width equal to 0.041 m, and tube thickness equal to 0.0014 m). The mass flow rate through tube is taken as 0.089 kg per seconds. Due to the symmetry of the geometry, a two-dimensional symmetric grid with 33,000 cells was generated from half of the geometry (Fig. 1). The grid independency test with a fine grid did not show realisable impact on the results. The time step for all studies was 0.1 seconds.

4. Numerical calculations

In the two processes of melting and solidification, the direction of the HTF flow was fixed and the temperature profile at the tube-PCM interface evolved as a steady boundary condition (SBC). In two other processes of melting and solidification, the flow direction of HTF was changed in specific time intervals which resulted in an oscillating temperature profile at the tube-PCM interface, or a periodic boundary condition (PBC). The specific time interval was calculated using a dimensional period (λ) that was proposed by Lage and Bejan (1993).

$$\lambda \sim 4 Z^2 Ra^{-0.4} / \alpha \quad Pr \geq 1 \quad (1)$$

Including $Ra = 10^{11}$, $\alpha = 1.65 \times 10^{-7}$ and $Z = 0.55$ in equation 1 results in $\lambda \approx 300$ seconds as the time of a complete cycle. From this calculation, the period of the reversing HTF flow was taken as 150 seconds.

Three domains of HTF, tube thickness and PCM were defined. The boundary conditions were set as symmetry at both sides of the geometry, adiabatic at the bottom and top of the PCM, HTF flow inlet at the top of the tube and HTF flow outlet at the bottom of the tube, as shown in Fig. 1. The HTF inlet temperature was set at 356.8°C for the melting processes, resulting in $T_h - T_m = 50^\circ\text{C}$. The inlet temperature for the solidification cases was set at 256.8°C , $T_m - T_c = 50^\circ\text{C}$. The initial temperature was set 5°C lower/higher (for melting/solidification respectively) than the PCM melting temperature ($T_m = 306.8^\circ\text{C}$) to distinguish the latent heat transfer stage after the preliminary stage of sensible heat transfer between the HTF and PCM.

5. Results and discussion

For the melting processes, results of temperature fields (isotherms) and phase fronts, mass and heat transfer, plus the phase change duration are compared for the two cases of steady and periodic boundary conditions at the tube-PCM interface. Moreover, the predicted temperature distribution and phase front, mass and heat fluxes and process time for the two solidification cases with steady and periodic boundary conditions are also compared.

5.1. Isotherms and phase fronts

In a phase change process, phase change occurs at the interface between the solid and liquid within a narrow region of melting temperature of the PCM. Therefore, temperature profiles or isotherms represent evolution of the phase change front where the latent heat transfer occurs. Thus, prediction of phase front, representing the heat transfer area between solid and liquid is considered highly important in understanding the thermal behavior of PCMs.

5.1.1. Melting processes

The temperature distribution in the PCM domain shows lower temperature gradients and lower peak temperatures for the periodic boundary condition at the tube-PCM interface compared to the steady one. Periodic HTF flow reversal prevents the continuous accumulation and temperature rise of the liquid PCM at the top, resulting in a more uniform temperature field and lower hot spots. This is shown in the Figs. 2a-f, representing three time slots and melt fractions (δl) in the two melting processes.

Lower peak temperatures and temperature gradients lead to lower entropy generation which ultimately enhances the exergy recovery of the system as mentioned in (Bejan, 2002). Table 1, shows the results of average entropy generation through the PCM in three different time slots for the cases with SBC and PBC. Less entropy generation is evident for the case with PBC with lower temperature gradient and lower peak temperatures.

Table 1. Comparison of average entropy generation, a) steady boundary condition, b) periodic boundary condition

time - seconds	a - J/kg. K	b - J/kg. K
2800	1212.8	1211.7
7000	1234.4	1224.6
12000	1274.3	1265.4

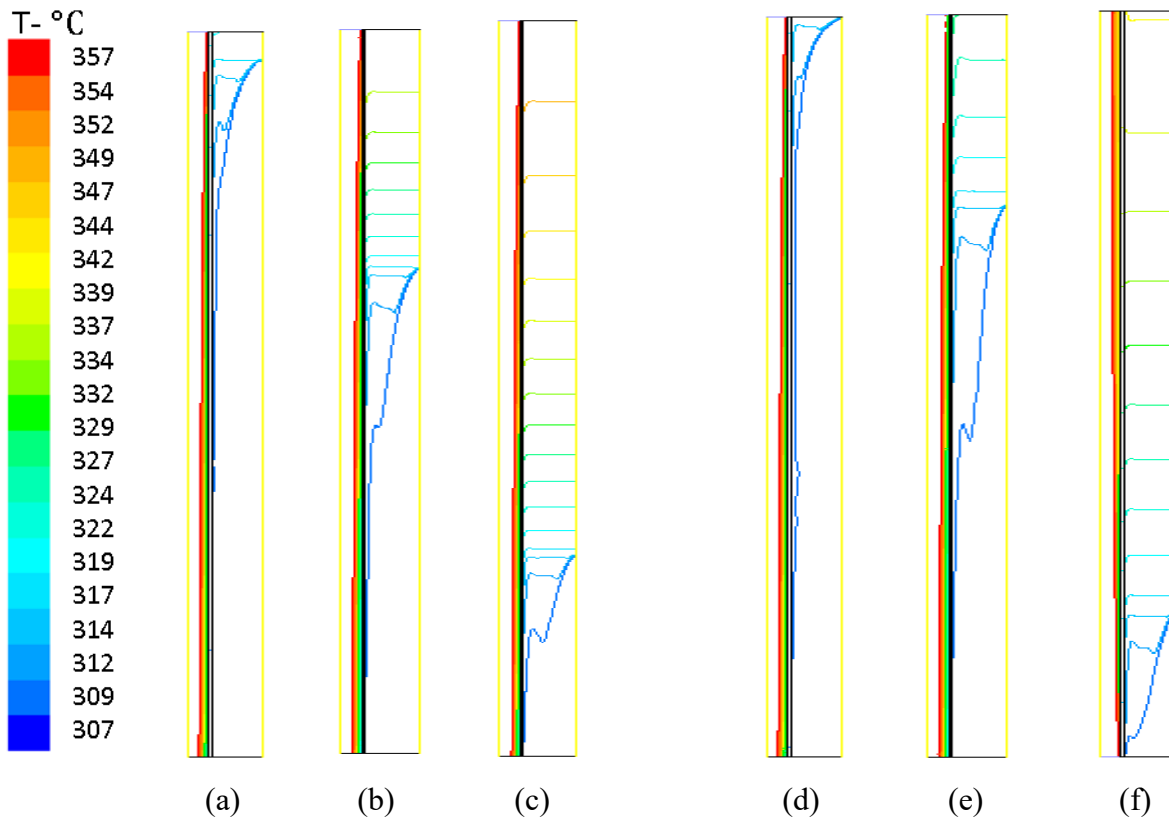


Figure 2. Isotherms evolution during melting processes, steady boundary:
a) 2800s, $\delta l = 25\%$, b) 7000s, $\delta l = 60\%$, c) 12000s, $\delta l = 86.6\%$, periodic boundary:
d) 2800s, $\delta l = 25\%$, e) 7000s, $\delta l = 63.6\%$, f) 12000s $\delta l = 92\%$.

5.1.2. Solidification processes

Fig. 3a-f represent the isotherms and phase fronts in the PCM domain for three time slots and solid fractions (δ_s) during two solidification processes. With the same trend as seen in the melting processes, lower temperature gradients are visible in Figs. 3d-e (periodic boundary at tube-PCM) compared with Figs. 3a-c (steady boundary). The mixing effect of the periodic reversal flow of HTF results in a more uniform temperature field compared to the case with the fixed flow direction of HTF during the whole process.

Considering other aspects, phase fronts in the solidification cases are one dimensional and evolve parallel to the tube throughout the whole process. However, due to the impact of periodic boundary condition at the tube-PCM interface, more uniform temperature distribution is found, and phase fronts are more uniform along the length (profiles in Fig. 3f compared to the profiles in Fig. 3c). Therefore, periodic flow reversal of HTF improves the heat transfer area as they evolve one dimensional and parallel to the tubes up to the end of process.

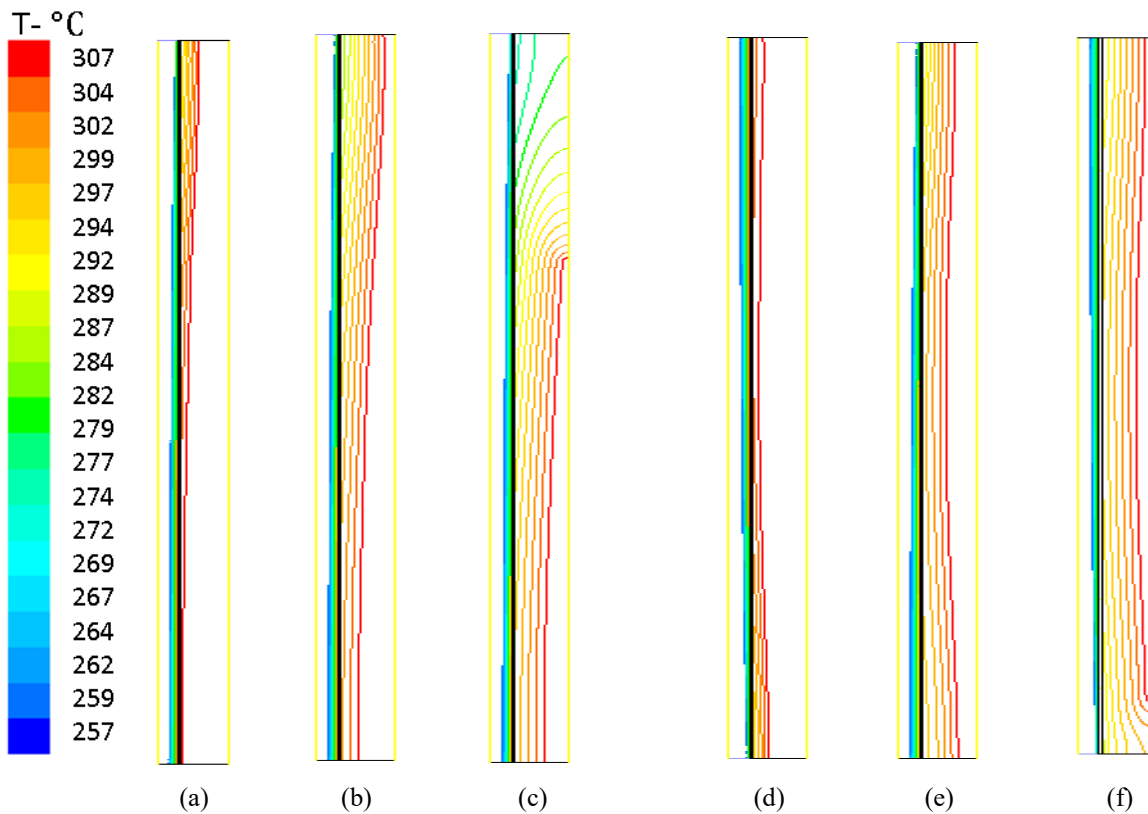


Figure 3. Isotherm evolution during solidification process, steady boundary:
a) 3000s, $\delta_s=28\%$, b) 7350s, $\delta_s=64\%$, c) 11000s, $\delta_s=86\%$, periodic boundary:
d) 3000s, $\delta_s=28\%$, e) 7350s, $\delta_s=64\%$, f) 11000s, $\delta_s=90\%$

5.2. Mass transfer

Table 2 shows the impact of periodic flow reversal of HTF on the mass transfer in the PCM domain after specific time periods. In the melting process with the SBC at the tube-PCM interface, the mass flux increases with the increasing of liquid fraction (δl) and decreases towards the end of the process as the temperature gradient through the PCM diminishes. However, implementing the periodic flow reversal of HTF, leads to resonance of convection heat transfer after 40% of PCM changes to the liquid phase, increasing the mass flux up to the end of process.

Table 2. Mass flux comparison, a) steady boundary condition, b) periodic boundary condition

time- seconds	a - kg/s	b - kg/s
2800	0.02	0.019
7000	0.0272	0.0367
12000	0.0193	0.0769

5.3. Heat transfer

The heat transfer enhancement of the periodic reversal of HTF flow can be seen in Figs. 4a, b. PBC at the tube-PCM interface due to the reversal of HTF flow leads to the resonance of convection heat transfer after 40% melt fraction in the charging process. This impact is clearly shown in Fig. 4a where the mean heat flux under PBC is about 6% higher than the melting process with the SBC. However, PBC at the tube-PCM interface leads to about 6% heat flux enhancement mainly at the later stages after 75% of phase change in the discharging process. Comparison of the phase change front being the heat transfer area in section 5.1.2 has shown higher heat transfer area for the discharging process under the PBC in comparison to the SBC after 75% solid fraction up to the end of process. Therefore, higher heat flux in the discharging process under the PBC is the result of higher heat transfer area at phase change front.

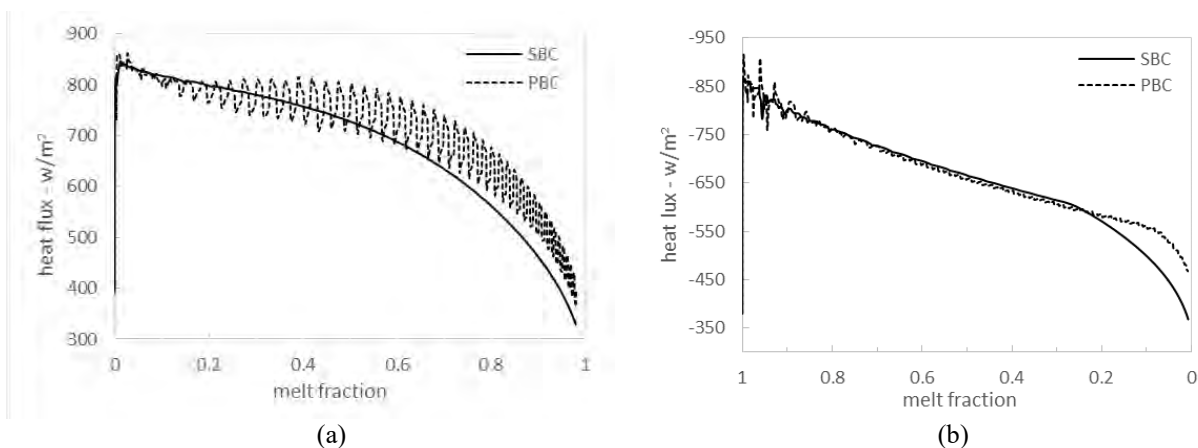


FIGURE 4. Temporal evolution of heat flux a) melting, b) solidification

5.4. Phase change time

Fig. 5 shows the impact of the implementation of HTF flow reversal on the phase change time. Periodic reversal of HTF flow direction decreases the phase change time in both the charging and discharging processes, about 10% and 12%, respectively. This is the result of heat transfer enhancement due to the resonance of convection heat transfer in the melting process and providing a higher heat transfer area at the later stages of the solidification process.

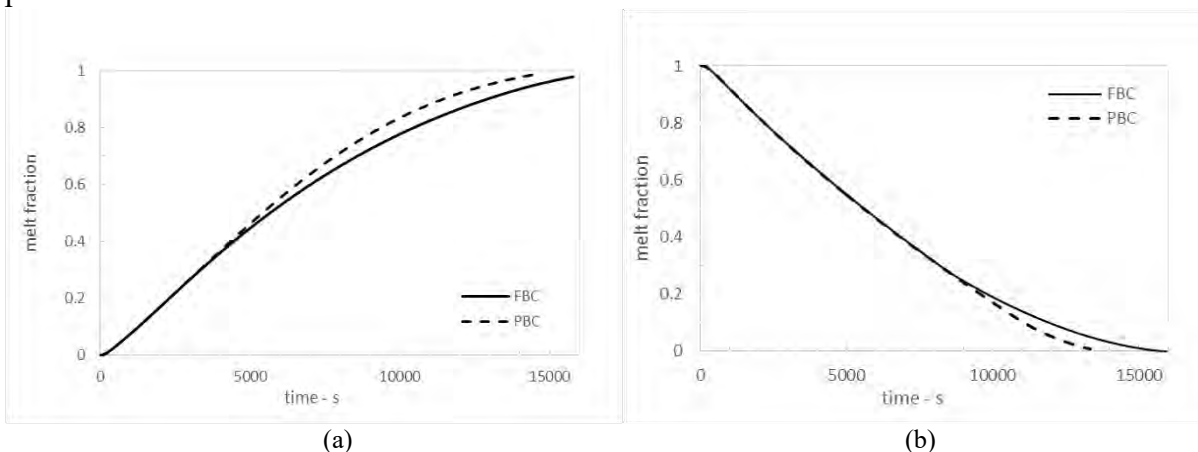


FIGURE 5. Temporal evolution of phase change a) melting, b) solidification

6. Conclusion

In this numerical study the impact of the periodic reversal of HTF flow on the mass and heat transfer, phase change front evolution and phase change time was investigated. The results have shown 6% heat transfer improvement due to resonance of convection heat transfer in the charging process. For the discharging process, the average heat flux increased by about 6% due to the higher heat transfer area as the impact of PBC on the evolution of phase change front.

In both charging and discharging processes, the imposed periodic boundary condition led to lower temperature gradient in space and time, and lower peak temperatures in the charging process.

The phase change time also decreased by about 10% and 12% under the PBC at the tube-PCM interface in the charging and discharging processes, respectively. This provides an opportunity for a LHTES unit being used in applications when higher power density is required, for instance high rates of heat storage is required to protect a receiver from overheating or fast release of heat is required during the peak demand in a CSP plant in response to a sudden change of solar irradiance. The reported improvements are considerable and need to be judged against the anticipated additional costs associated with the provision of a system capable of providing the means for periodic flow reversal.

References

- ANSYS Fluent Users Guide, Release 15.0, 2015, ANSYS.
- Antohe, B.V. and Lage J.L., 1996, 'Experimental Investigation on Pulsating Horizontal Heating of a Water-Filled Enclosure', *Journal of Heat Transfer*, 118(4), p889-896.
- Antohe, B.V. and Lage J.L., 1996, 'Amplitude effect on convection induced by time-periodic horizontal heating', *International Journal of Heat and Mass Transfer*, 39(6): p1121-1133.
- Antohe, B.V. and Lage J.L., 1997, 'The Prandtl number effect on the optimum heating frequency of an enclosure filled with fluid or with a saturated porous medium', *International Journal of Heat and Mass Transfer*, 40(6), p1313-1323.
- Bejan, A., Fundamentals of exergy analysis, entropy generation minimization, and the generation of flow architecture. *International Journal of Energy Research*, 2002. 26(7): p. 0-43.
- Ho, C.J. and C.H. Chu, 1993, 'Periodic melting within a square enclosure with an oscillatory surface temperature', *International Journal of Heat and Mass Transfer*, 36(3), p725- 733.
- Ho, C.J. and C.H. Chu, 1993, 'The melting process of ice from a vertical wall with time-periodic temperature perturbation inside a rectangular enclosure', *International Journal of Heat and Mass Transfer*, 36(13), p3171-3186.
- Jones, B.J., Sun D., Krishnan S., and Garimella S.V., 2006, 'Experimental and numerical study of melting in a cylinder'. *International Journal of Heat and Mass Transfer*, 49(15), p2724-2738.
- Krishnan, S., Murthy J.Y., and Garimella S.V., 2006, 'Analysis of Solid-Liquid Phase Change Under Pulsed Heating', *Journal of Heat Transfer*, 129(3), p395-400.
- Lage, J.L. and Bejan A., 1993, 'The resonance of natural convection in an enclosure heated



periodically from the side', *International Journal of Heat and Mass Transfer*, 36(8), p2027-2038.

Lan, C.W. and D.T. Yang, 1998, Dynamic simulation of the vertical zone-melting crystal growth, *International Journal of Heat and Mass Transfer*, 41(24), p4351-4373.

Riahi, S., Saman W.Y., Bruno F., Tay N.H.S., 2016, 'Numerical modeling of inward and outward melting of high temperature PCM in a vertical cylinder', *AIP Conference Proceedings*, 1734, 050039.

Voller, V.R., Brent A., and Prakash C., 1989, 'The modelling of heat, mass and solute transport in solidification systems', *International Journal of Heat and Mass Transfer*, 32(9), p1719-1731.

Acknowledgements

The Authors gratefully acknowledge that this work is part of the Australian Solar Thermal Research Initiative (ASTRI) project supported by the Australian Government through the Australian Renewable Energy Agency (ARENA).

Nomenclature

c	specific heat, J/kg.K
L	latent heat of fusion, J/kg
Pr	Prndtl number, ν/α
Ra	Rayleigh number, $g\beta Z^3(T_h - T_m)/\nu\alpha$
Ste	Stefan number, $c_l(T_h - T_m)/L$
T	temperature, °C
Z	height of enclosure, m

Greek Symbols

α	thermal diffusivity, m^2/s
β	thermal expansion coefficient, 1/K
δ_l, δ_s	liquid/solid fraction
ν	kinematic viscosity, m^2/s
λ	dimensional period, s

Subscript

c	cold wall
h	hot wall
l	liquid
m	melting